# Wnt5a cooperates with canonical Wnts to generate midbrain dopaminergic neurons in vivo and in stem cells

Emma R. Andersson[a,b,1], Carmen Saltó[a,1], J. Carlos Villaescusa[a], Lukas Cajanek[a], Shanzheng Yang[a], Lenka Bryjova[a,c,d], Irina I. Nagy[e], Seppo J. Vainio[e], Carmen Ramirez[a,f], Vitezslav Bryja[a,c,d], and Ernest Arenas[a,2]

[a]Laboratory of Molecular Neurobiology, Department of Medical Biochemistry and Biophysics, Center of Developmental Biology for Regenerative Medicine, and [b]Department of Cell and Molecular Biology, Karolinska Institute, Stockholm, 171 77 Sweden; [c]Department of Cytokinetics, Institute of Biophysics, Academy of Sciences of the Czech Republic, and [d]Institute of Experimental Biology, Faculty of Science, Masaryk University, 611 37, Brno, Czech Republic; [e]Biocenter Oulu, Oulu Center for Cell Matrix Research, Department of Medical Biochemistry and Molecular Biology, University of Oulu, 90014, Oulu, Finland; and [f]Laboratory of Cellular and Molecular Biology of Stem Cells, Centro Regional de Investigaciones Biomédicas, Universidad de Castilla La Mancha, 02006 Albacete, Spain

Edited by Thomas C. Südhof, Stanford University School of Medicine, Stanford, CA, and approved December 12, 2012 (received for review May 20, 2012)

**Wnts are a family of secreted proteins that regulate multiple steps of neural development and stem cell differentiation. Two of them, Wnt1 and Wnt5a, activate distinct branches of Wnt signaling and individually regulate different aspects of midbrain dopaminergic (DA) neuron development. However, several of their functions and interactions remain to be elucidated. Here, we report that loss of *Wnt1* results in loss of Lmx1a and *Ngn2* expression, as well as agenesis of DA neurons in the midbrain floor plate. Remarkably, a few ectopic DA neurons still emerge in the basal plate of *Wnt1*$^{-/-}$ mice, where Lmx1a is ectopically expressed. These results indicate that *Wnt1* orchestrates DA specification and neurogenesis in vivo. Analysis of *Wnt1*$^{-/-}$;*Wnt5a*$^{-/-}$ mice revealed a greater loss of Nurr1$^{+}$ cells and DA neurons than in single mutants, indicating that *Wnt1* and *Wnt5a* interact genetically and cooperate to promote midbrain DA neuron development in vivo. Our results unravel a functional interaction between *Wnt1* and *Wnt5a* resulting in enhanced DA neurogenesis. Taking advantage of these findings, we have developed an application of Wnts to improve the generation of midbrain DA neurons from neural and embryonic stem cells. We thus show that coordinated Wnt actions promote DA neuron development in vivo and in stem cells and suggest that coordinated Wnt administration can be used to improve DA differentiation of stem cells and the development of stem cell-based therapies for Parkinson's disease.**

ES cell | Wnt3a | Mash1 | Foxa2 | Pitx3

Wnts are a large family of lipid-modified glycoproteins that are evolutionarily conserved and serve multiple functions in development, tissue homeostasis, and disease (1–3). These proteins work as ligands that bind to and activate a growing number of membrane-bound receptors that in turn activate numerous signaling pathways, including Wnt/β-catenin, Wnt/planar cell polarity (PCP)/small GTPase, and Wnt/$Ca^{2+}$ pathways (4–6). By activating several of these pathways, Wnts control a wide variety of essential functions in diverse tissues, including the nervous system. For example, Wnts are known to control neural patterning, morphogenesis, polarity, proliferation, differentiation, survival, neuritogenesis, axonogenesis, and synaptogenesis (3, 7–12).

Several Wnts and their signaling components are expressed in the developing ventral midbrain (VM) (13–15). These include Wnt1, Wnt2, and Wnt3a, which activate the Wnt/β-catenin pathway (14, 16), and Wnt5a, which activates the Wnt/Rac1 pathway in dopaminergic (DA) cells (17). *Wnt1*-knockout mice show a partial segmental deletion of the midbrain and hindbrain regions (18, 19) resulting from multiple sequential defects, including altered Otx2 and Pitx3 expression, reduced progenitor proliferation, and death of midbrain DA neurons (18–22). This phenotype is in stark contrast with the phenotype of the *Wnt5a*$^{-/-}$ mice, in which progenitor proliferation is enhanced, Nurr1$^{+}$ precursors are in excess, and a nearly normal number of tyrosine hydroxylase-positive (TH$^{+}$) cells are mispositioned by a convergent extension defect [lateral expansion and anterior–posterior (A–P) shortening of the VM] (17). Similarly, in vitro studies have shown that Wnt1 activates Wnt/β-catenin signaling and regulates the expression of Lmx1a and Otx2 in mouse ES cells (23) and acts on DA progenitors to promote proliferation and (to a lesser extent) DA differentiation (14, 24, 25). In contrast, Wnt5a, a Wnt that activates Wnt/Rac1 signaling in DA cells, promotes VM morphogenesis and DA differentiation (17, 26). We, and others, have shown that canonical Wnts such as Wnt1 or Wnt3a activate Wnt/β-catenin signaling and promote midbrain DA neurogenesis both in vitro (24, 27, 28), and in vivo (29, 30), in part by negatively regulating Sonic hedgehog (Shh) in the midbrain floor plate (FP) (30–32). However, it also has been reported that an excess of Wnt/β-catenin signaling leads to a defect in the differentiation of Nurr1$^{+}$ DA neuroblasts and a decrease in the number of midbrain DA neurons (32). These results indicate that the level of Wnt/β-catenin signaling is critical in regulating DA neuron development. Surprisingly, the defect generated by overactivation of Wnt/β-catenin signaling is not rescued by administration of Shh but instead is rescued by Wnt5a (32). These data led us to hypothesize that Wnt/β-catenin signaling may need to be in balance with Wnt5a, at least during DA precursor differentiation. To test this hypothesis, we examined whether *Wnt1* and *Wnt5a* interact genetically and compete functionally or cooperate to generate midbrain DA neurons in vivo. Our analysis of *Wnt1*$^{-/-}$;*Wnt5a*$^{-/-}$ mice revealed, first, that *Wnt1* is the Wnt required for midbrain DA specification and neurogenesis and, second, that *Wnt1* and *Wnt5a* interact genetically and cooperate to promote midbrain DA neurogenesis in vivo. Based on these findings, we developed a Wnt protocol that improves the DA differentiation of both neural and ES cells.

Author contributions: E.R.A., C.S., J.C.V., L.C., C.R., V.B., and E.A. designed research; E.R.A., C.S., J.C.V., L.C., S.Y., L.B., and C.R. performed research; I.I.N. and S.J.V. contributed new reagents/analytic tools; E.R.A., C.S., J.C.V., L.C., S.Y., C.R., V.B., and E.A. analyzed data; and E.R.A. and E.A. wrote the paper.

The authors declare no conflict of interest.

This article is a PNAS Direct Submission.

Freely available online through the PNAS open access option.

[1]E.R.A. and C.S. contributed equally to this work.

[2]To whom correspondence should be addressed. E-mail: Ernest.Arenas@ki.se.

See Author Summary on page 2450 (volume 110, number 7).

This article contains supporting information online at www.pnas.org/lookup/suppl/doi:10.1073/pnas.1208524110/-/DCSupplemental.

We suggest that differentiation protocols incorporating critical aspects of both Wnt/β-catenin–dependent and –independent pathways can contribute to current efforts to develop stem cell-based therapies for Parkinson's disease.

## Results

***Wnt1* Is Required for DA Neurogenesis and to Specify the Midbrain FP as a Neurogenic Region.** Recent reports have indicated that Wnt/β-catenin signaling is required for midbrain DA neurogenesis (30, 31), but it is not known which of the multiple canonical Wnts expressed in the VM (13–15) is/are required for DA neurogenesis. In our study we focused on Wnt1 because *Wnt1*$^{-/-}$ mice, unlike *Wnt2*$^{-/-}$ mice, for instance (16), show a strong sequential midbrain and DA neuron phenotype (18–22). Because DA neurons are born in the midbrain FP, we first examined the expression of the FP and basal plate (BP) markers, *Shh* and the *Shh*-target gene, *Foxa2,* both of which are required for DA neuron development (31, 33–35). In situ hybridization (ISH) revealed that the expression patterns of *Shh* and *Foxa2* were delayed, as previously described in *β-catenin*$^{-/-}$ mice (31). Indeed, we found a delay in the lateral expansion of the *Shh* and *Foxa2* expression domains (Fig. 1*A*, asterisks) and in the down-regulation of *Shh* in the FP (Fig. 1*A*, arrow), as well as weaker levels of *Foxa2* in *Wnt1*$^{-/-}$ mice at embryonic day (E) 11.5 (Fig. 1*A*). Surprisingly, no TH$^{+}$ DA neurons were present in the FP of *Wnt1*$^{-/-}$ mice at E12, and only a few DA neurons arose in an ectopic lateral position in the Foxa2$^{+}$ BP, which at this stage showed normal Foxa2 protein levels (Fig. 1*B*). Moreover, Lmx1a, a Lim homeobox transcription factor required for the specification of DA neurons (36), was also absent from the FP and was ectopically expressed in the BP of *Wnt1*$^{-/-}$ mice at E11.5 (Fig. 1*C*). Previous in vitro experiments have indicated that β-catenin regulates Lmx1a via an auto-regulatory loop (23) and that deletion of β-catenin results in ectopic expression of Lmx1a in vivo (30). Because Wnt1 activates Wnt/β-catenin signaling, our results indicate that it is Wnt1 that regulates the expression levels and position of Lmx1a in vivo. Interestingly, examination of the lateral Lmx1a$^{+}$ BP region revealed that it is the site where the few midbrain DA neurons are present in *Wnt1*$^{-/-}$ mice (Fig. 1*C*). We therefore asked whether the lateral displacement of Lmx1a$^{+}$ and TH$^{+}$ cells results from an inversion of the BP and FP domains and examined the expression and distribution of Nkx6.1, which normally is expressed in the BP and alar plate of the midbrain (33, 37). Although a partial reduction in the number of Nkx6.1$^{+}$ cells was detected at E11.5 and E12.5 (Fig. S1*A*), Nkx6.1$^{+}$ cells were found laterally, in the correct position. Similarly, the expression pattern of Wnt5a in the medial and basal plates of the VM was not disrupted in *Wnt1*$^{-/-}$ mice at E11.5 (Fig. S1*B*). These results, together with the medial expression of *Shh* and *Foxa2* (Fig. 1*A*), indicated that the midbrain FP and BP domains were not inverted in *Wnt1*$^{-/-}$ mice but that gene expression in these compartments is altered.

Because the midbrain FP contained no Lmx1a$^{+}$ or TH$^{+}$ cells, we then asked whether overall neurogenesis was impaired and examined the expression of proneural genes in the VM FP of *Wnt1*$^{-/-}$ mice at E11.5. We have shown previously that *Ngn2* is required for DA neuron development and can be partially replaced by *Mash1* (38). Interestingly, the expression of both *Ngn2* and *Mash1* was abolished in the midbrain FP, and *Ngn2* expression increased in the dorsal midbrain and particularly in the BP of *Wnt1*$^{-/-}$ mice (Fig. 1*D*). These results suggested that Wnt1 controls neurogenesis in the midbrain and led us to examine whether any neurons are found in the FP of *Wnt1*$^{-/-}$ mice. Staining with Topro3 (a nuclear marker) first revealed that the WT midbrain FP consisted of nearly 20 cell diameters in the midline (in ventricular, intermediate, and marginal zones) at E12.5, whereas only about five cell diameters (in the ventricular zone) were found in *Wnt1*$^{-/-}$ mice (Fig. 1*E*). Staining for Tuj1, a pan-neuronal marker, and Topro3, a nuclear marker, revealed no double Tuj$^{+}$/Topro$^{+}$ cell bodies in the FP, indicating that the FP region of *Wnt1*$^{-/-}$ mice contains no newborn neurons and that only commissural Tuj1$^{+}$ fibers are present (Fig. 1*E*). Moreover, no Nurr1$^{+}$ DA neuroblasts were detected in the FP. In fact, the only cell bodies found in the FP of *Wnt1*$^{-/-}$ mice were those of Sox2$^{+}$ ventricular zone neuroepithelial cells (Fig. 1*F*) and Glast$^{+}$ radial glia (22). Interestingly, a reduced number of Nurr1$^{+}$ DA neuroblasts also were found in an ectopic lateral position in the BP (Fig. 1*F*). Thus, our results indicate that Wnt1 is required not only for the expression of Lmx1a and proneural genes (*Mash1* and *Ngn2*) in the midbrain FP but also for DA specification and neurogenesis.

**Wnt1 and Wnt5a Interact Genetically to Regulate the Development of Midbrain DA Neurons.** To investigate whether Wnt1 interacts genetically and functionally with Wnts that activate Wnt/PCP signaling and regulate midbrain DA neuron development, we generated double *Wnt1*$^{-/-}$;*Wnt5a*$^{-/-}$ mice. We chose *Wnt5a*$^{-/-}$ mice because deletion of *Wnt11*, another Wnt capable of activating Wnt/PCP signaling, did not induce any detectable change in the number or position of midbrain DA neurons at E11.5 or E14.5 (Fig. S2). *Wnt1*$^{-/-}$*Wnt5a*$^{+/+}$ mice showed a partial deletion of the midbrain/hindbrain region (Fig. 2*A*), as previously shown for *Wnt1*$^{-/-}$ mice (18–22). On the other hand, *Wnt1*$^{+/+}$;*Wnt5a*$^{-/-}$ mice displayed the typical flattening of the midbrain FP region and a shortening of the A–P axis (17, 39), which was very obvious in the tail region at E10.5 (Fig. 2*A*). Interestingly, *Wnt1*$^{-/-}$*Wnt5a*$^{-/-}$ compound knockouts resembled a combination of the two phenotypes and showed exacerbated caudal phenotypes, a shortened and truncated midbrain, and a flattening of the FP region (Fig. 2 *A* and *B*).

We then performed a detailed analysis of the VM, starting by examining the proliferation of VM progenitors in *Wnt1*/*Wnt5a* double -mutant mice. Previous studies have indicated that deletion of *Wnt1* reduces (22) but deletion of *Wnt5a* increases (17) progenitor proliferation in the midbrain FP. However, it is not known whether these two Wnts interact to regulate proliferation in vivo. Although no difference in phospho-histone 3 (PH3) staining (for cells in M-phase) was detected in the BP of *Wnt1*$^{-/-}$ or *Wnt1*$^{-/-}$;*Wnt5a*$^{-/-}$ mice, significant and specific changes were detected in the FP. Indeed, deletion of *Wnt5a* in *Wnt1*$^{-/-}$;*Wnt5a*$^{-/-}$ mice rescued the *Wnt1*$^{-/-}$ FP loss of PH3$^{+}$ cells by 40% and increased PH3 by 2.5-fold, compared with Wnt1$^{-/-}$ mice (Fig. 2 *B* and *C*). This increase was much more pronounced than the 20% increase in mitotic cells in *Wnt5a*$^{-/-}$ single-mutant mice (17). Thus, our results indicate that Wnt5a serves a stronger proliferative role in the absence of endogenous Wnt1 and that *Wnt1* and *Wnt5a* interact in an antagonistic manner to regulate proliferation in vivo. We then asked whether this partial rescue of proliferation leads to an increase in the number of Nurr1$^{+}$ postmitotic cells in *Wnt1*$^{-/-}$;*Wnt5a*$^{-/-}$ mice through increased neurogenesis, as shown previously for *Wnt5a*$^{-/-}$ mice (17). This was not the case, because deletion of *Wnt5a* in *Wnt1*$^{-/-}$ mice resulted in a greater loss of the total number of Nurr1$^{+}$ cells in the VM BP, from a 57% reduction in *Wnt1*$^{-/-}$;*Wnt5a*$^{+/+}$ mice to an 81% reduction in *Wnt1*$^{-/-}$;*Wnt5a*$^{-/-}$ mice (Fig. 2*D*). These results indicated that Wnt1 and Wnt5a cooperate in the generation of postmitotic cells and prompted us to examine the number of TH$^{+}$ DA neurons in the VM of *Wnt1*$^{-/-}$;*Wnt5a*$^{-/-}$ mice. We have shown previously that the loss of *Wnt5a* does not decrease the number of DA neurons (17), whereas others have shown that deletion of *Wnt1* dramatically decreases the number of DA neurons (22). Here, we found that deletion of *Wnt5a* in *Wnt1*$^{-/-}$ mice led to a nearly complete loss of TH$^{+}$ cells at E12.5 (Fig. 2 *E* and *F*, *Lower*), indicating that, as in the case of Nurr1, *Wnt5a* worsens the *Wnt1* phenotype and cooperates positively with *Wnt1* to regulate DA neurogenesis. Moreover, although

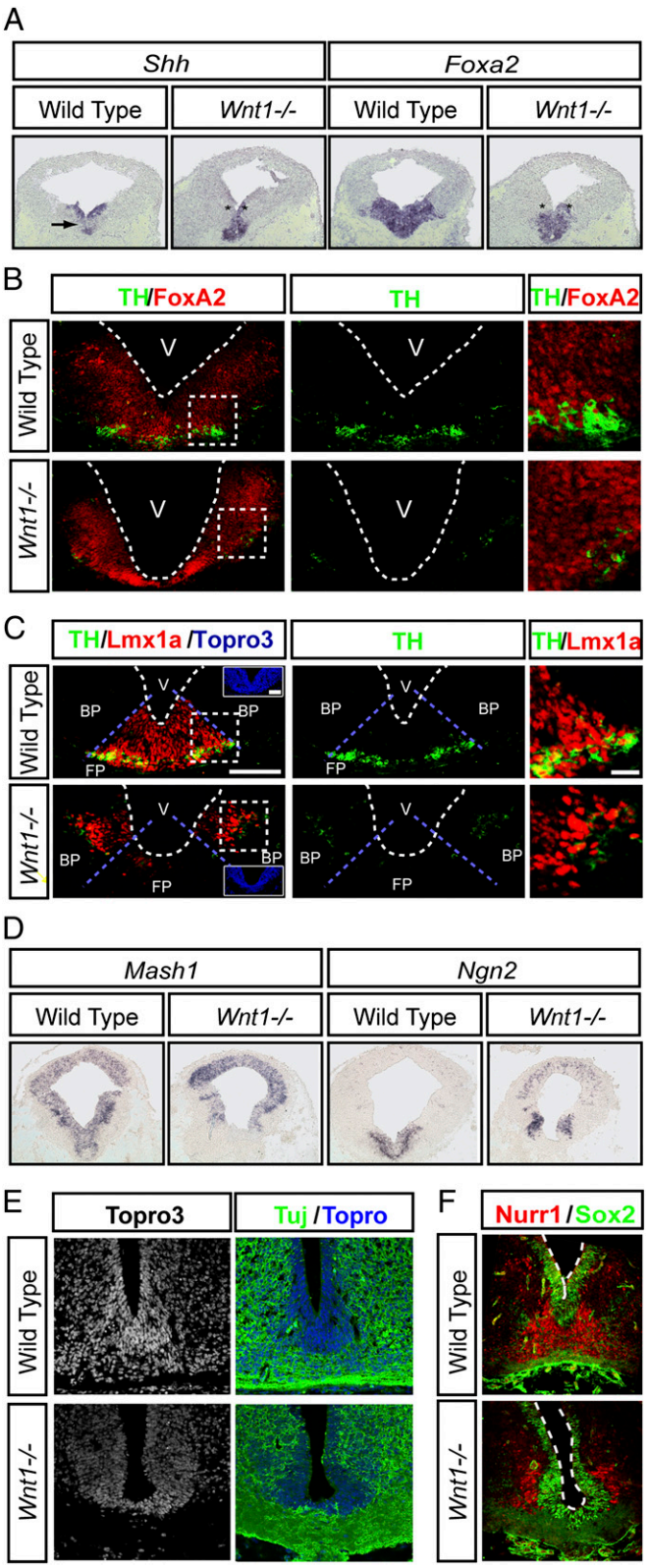


**Fig. 1.** Wnt1 is required for ventral midbrain FP neurogenesis. (*A*) *Shh* and *Foxa2* mRNA expression in the VM of *Wnt1*$^{-/-}$ mice is delayed compared with WT mice at E11.5; their expression is lost in lateral positions (*), and the medial down-regulation of *Shh* in WT mice (arrow) is not detected in *Wnt1*$^{-/-}$ mice. (*B*) Foxa2 protein and TH are found throughout the VM of WT mice at E12, whereas TH$^{+}$ DA neurons are severely reduced in number and are found solely in the lateral BP in *Wnt1*$^{-/-}$ mice. The boxed regions in the left panels demarcate the regions that are magnified in the panels at the far right. V = ventricle. (*C*) TH$^{+}$ cells are found only in Lmx1a$^{+}$ domains, which are laterally displaced from the FP to the BP in *Wnt1*$^{-/-}$ mice. The boxed regions in the left panels demarcate the regions that are magnified in the panels at the far right. (*D*) The expression of the proneural factors *Mash1* and *Ngn2* is lost from the FP and is displaced laterally in *Wnt1*$^{-/-}$ mice at E11.5. (*E*) At E12.5, the FP of *Wnt1*$^{-/-}$ mice shows a reduced ventricular zone and contains no neuronal somas (Tuj$^{+}$Topro3$^{+}$ cells). (*F*) Although the WT FP contains Sox2$^{+}$ progenitors and Nurr1$^{+}$ postmitotic cells, the *Wnt1*$^{-/-}$ FP shows fewer Sox2$^{+}$ progenitors, and all Nurr1$^{+}$ cells are found in the BP.

Nurr1$^{+}$, TH$^{+}$, or Lmx1a$^{+}$ cells always were found in the midbrain FP of WT mice, none of them were present in the FP of *Wnt1*$^{-/-}$*Wnt5a*$^{+/+}$, or *Wnt1*$^{-/-}$*Wnt5a*$^{-/-}$ mice. Combined, these data show that *Wnt1* and *Wnt5a* interact genetically in a complex manner resulting in both antagonistic and synergistic functions in the developing VM, as shown by the opposing regulation of proliferation and the cooperative regulation of DA neurogenesis by *Wnt1* and *Wnt5a*.

The phenotype described above showed that deletion of *Wnt5a* aggravates the neurogenesis phenotype of *Wnt1*$^{-/-}$ mice. Therefore we next decided to examine whether the opposite also is true, i.e., whether deletion of *Wnt1* worsens typical *Wnt5a*$^{-/-}$ phenotypes such as morphogenesis defects caused by alterations in convergent extension. We previously have reported that deletion of *Wnt5a* leads to a broadening of the ventricular cavity at the midbrain level that results in a flattening of the ventricular hinge point of the VM (17). Here we found that deletion of *Wnt1* leads to the opposite phenotype, an elongation of the ventricular cavity and of the VM hinge point. Interestingly, compound *Wnt1*$^{-/-}$;*Wnt5a*$^{-/-}$ mutants showed a *Wnt5a*$^{-/-}$-like phenotype, with a severe broadening of the ventricular cavity and flattening of the VM hinge point (Fig. 2*F*, arrows). We next examined whether other Wnt5a morphogenesis phenotypes, such as the 15% reduction in the A–P length of the TH$^{+}$ domain (17), were modified in *Wnt1*$^{-/-}$;*Wnt5a*$^{-/-}$ mice. Surprisingly, we found that the A–P distribution of the TH$^{+}$ midbrain DA domain, which was shortened by 55% in *Wnt1*$^{-/-}$ mice (Fig. 2*G*), was reduced further by 85% in *Wnt1*$^{-/-}$;*Wnt5a*$^{-/-}$ mice (Fig. 2*G*). Moreover, when the mediolateral and dorsoventral axes were examined, TH$^{+}$ cells occupied more lateral and dorsal positions in the *Wnt1*$^{-/-}$;*Wnt5a*$^{-/-}$ mice than in either of the single mutants (arrowheads in Fig. 2*F*). Thus, our data show that the combined deletion of *Wnt1* and *Wnt5a* results in a greater alteration of convergent extension (shorter A–P domain as well as lateral and ventral DA cell distribution), indicating that *Wnt1* cooperates positively with *Wnt5a* in regulating morphogenetic movements in the midbrain.

In sum, our results show a complex interaction between *Wnt5a* and *Wnt1* in which the function of *Wnt5a* in morphogenesis is potentiated by *Wnt1,* and the function of *Wnt1* in neurogenesis, but not in proliferation, is potentiated by *Wnt5a*. We thus decided to examine whether combined administration of Wnt proteins to stem cells, at the right time point of differentiation and in the correct sequence, could be used to improve current protocols for the DA differentiation of both neural stem cells and ES cells.

**Wnts Cooperate to Improve DA Neuron Development in Neural Stem Cells.** *Wnt1* overexpression or Wnt1-conditioned media have been used previously to activate Wnt/β-catenin signaling (40–42) and to promote DA differentiation of midbrain progenitors (14) or mouse ES (mES) cells (23). However, to date, it has not been possible to obtain pure Wnt1 protein capable of activating Wnt/β-catenin signaling. Indeed, Wnt1 protein (purified by us or commercially available) did not activate Wnt/β-catenin signaling, as assessed by diverse assays such as Lrp6 phosphorylation, dephosphorylation of β-catenin, or activation of the TOPFLASH

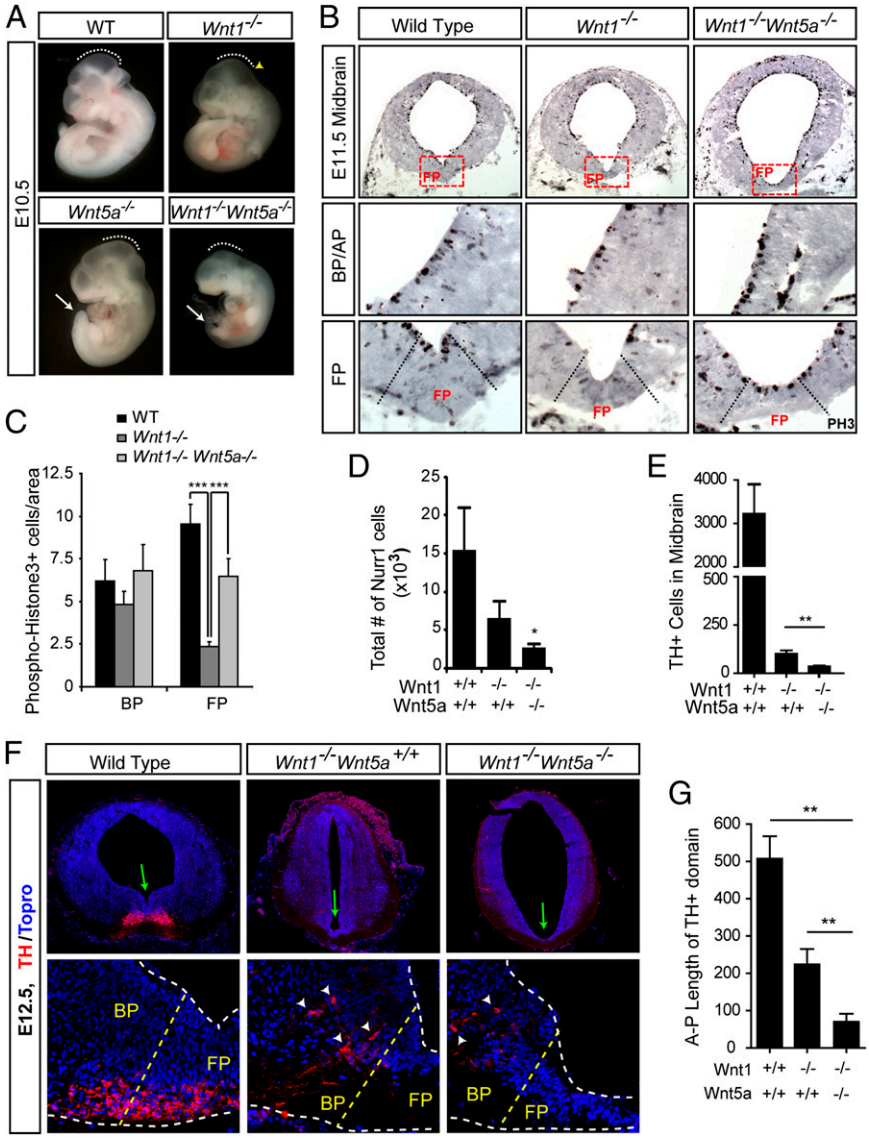


**Fig. 2.** Wnt1/Wnt5a double-mutant mice reveal redundant and nonredundant functions during ventral midbrain development. (*A*) *Wnt1*$^{+/-}$;*Wnt5a*$^{+/-}$ mice were mated to produce WT, *Wnt1*$^{-/-}$;*Wnt5a*$^{+/+}$ (labeled *Wnt1*$^{-/-}$), *Wnt1*$^{+/+}$;*Wnt5a*$^{-/-}$ (labeled *Wnt5a*$^{-/-}$), and *Wnt1*$^{-/-}$;*Wnt5a*$^{-/-}$ mice. At E10.5, *Wnt1*$^{-/-}$ mice display the previously described phenotypes of midbrain deletion and a less distinct isthmus (yellow arrowhead), whereas *Wnt5a*$^{-/-}$ mice display A–P shortening which is most obvious in the tail region (white arrow). *Wnt1*$^{-/-}$;*Wnt5a*$^{-/-}$ double-mutant mice resemble a combination of the two single knockouts, with a shortened A–P axis and a significantly shorter midbrain region (dashed lines). (*B* and *C*) Proliferation, assessed by staining for the mitotic marker PH3, is specifically reduced in the FP but not the BP of *Wnt1*$^{-/-}$ mice. Panels show whole midbrain (*Top Row*) and magnifications of the BP and FP (*Middle Row*). The areas demarcated by red dotted boxes are magnified in the bottom row. The reduction in the numbers of PH3$^{+}$ cells in the FP of *Wnt1*$^{-/-}$ mice is partially rescued by loss of *Wnt5a*. (*D*) The total number of Nurr1$^{+}$ cells decreases to a greater extent in double mutants than in single mutants or WT littermates. (*E* and *F*) TH$^{+}$ cells are dramatically reduced in number and are laterally displaced (white arrowheads in *F*) from the FP to the BP in *Wnt1*$^{-/-}$;*Wnt5a*$^{+/+}$ mice. These defects are worsened in *Wnt1*$^{-/-}$;*Wnt5a*$^{-/-}$ mice, in which even fewer cells are found (*E*), and they are positioned further dorsolaterally in the BP (white arrowheads in *F*). The VM hinge point (invagination of the ventricle; green arrow in *F*) is elongated in *Wnt1*$^{-/-}$ *Wnt5a*$^{+/+}$ mice and flattened in *Wnt1*$^{-/-}$;*Wnt5a*$^{-/-}$ mice. (*G*) The decrease of the A–P length of the TH-expressing midbrain domain observed in *Wnt1*$^{-/-}$ mice is exacerbated by loss of *Wnt5a*. $^{*}P < 0.05$, $^{**}P < 0.01$, $^{***}P < 0.001$.

reporter in DA cells (Fig. S3). This lack of activation is in contrast with other purified Wnt proteins such as Wnt3a or Wnt5a, which have been shown to activate Wnt signaling and to exert biologically relevant activities (26, 43). Given the current unavailability of purified active Wnt1 protein for our experiments, we turned our attention to Wnt3a, a protein capable of activating Wnt/β-catenin signaling in DA cells (Fig. S3) (14). We thus examined whether it was possible to substitute Wnt1 for Wnt3a as a source of Wnt/β-catenin activation in our stem cell-differentiation protocols. We started by devising a three-step protocol to treat midbrain progenitor/neural stem cells, expanded as neurospheres (Fig. 3*A*), in which we first used Wnt3a for 3 d to promote progenitor proliferation and specification, followed by 3 d without Wnts to eliminate all remaining Wnt3a, and finally 3 d with Wnt5a to activate the Wnt/PCP/Rac1 pathway, promote progenitor cell-cycle exit, and direct Nurr1$^{+}$ precursor differentiation into TH$^{+}$ DA neurons (17). Although treatment with Wnt3a alone at the indicated time point (Fig. 3*A*) increased the number of TuJ1$^{+}$ neurons, Wnt5a alone or Wnt3a and Wnt5a did not affect the number of neurons in the culture (Fig. 3 *B*,

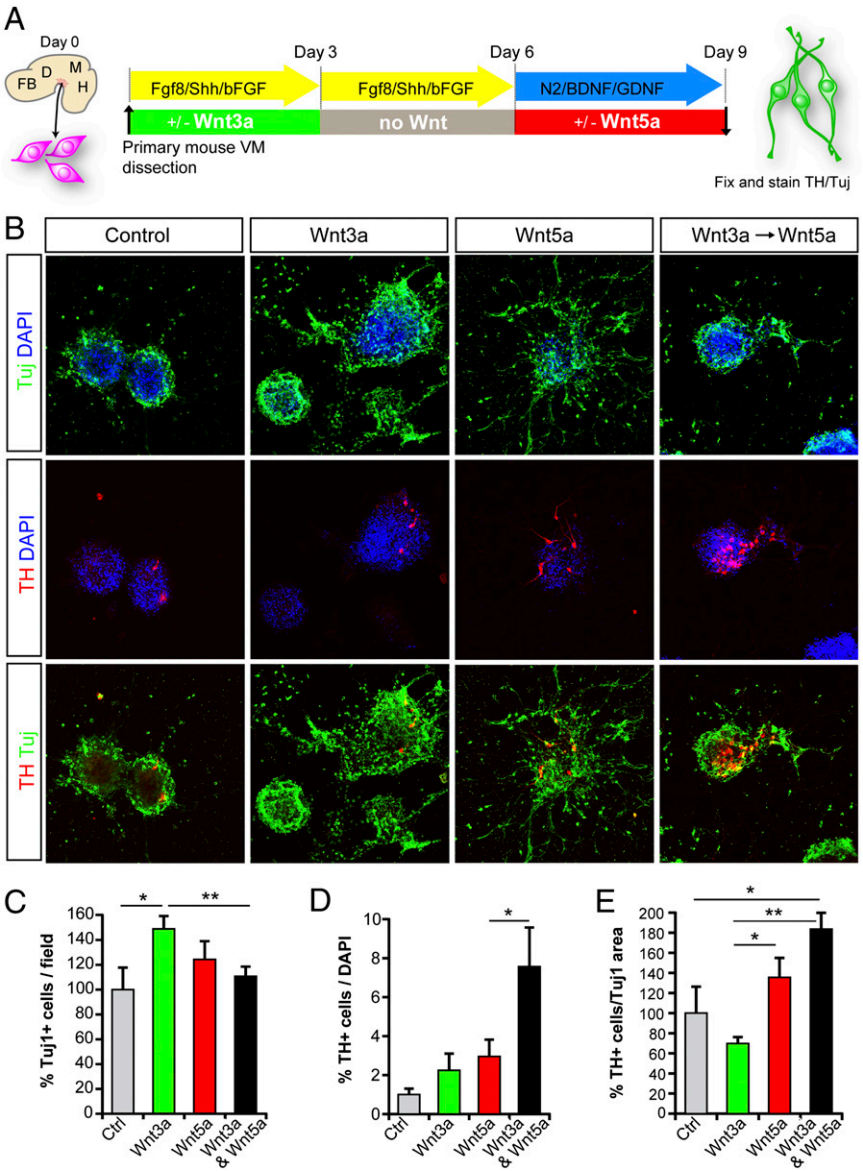


**Fig. 3.** Sequential Wnt3a and Wnt5a treatment of primary ventral midbrain neurospheres improves the yield of DA neurons. (*A*) Mouse E11.5 VM cultures were grown for the first 6 d in the presence of FGF8b (25 ng/mL), Shh (300 ng/mL), and bFGF (20 ng/mL). Wnt3a was added during the first 3 d, and Wnt5a was added during days 6–9, in the presence of BDNF (20 ng/mL) and GDNF (10 ng/mL). (*B*) Immunocytochemistry for TUJ1/DAPI, TH/DAPI, and TH/TUJ1 revealed that Wnt3a increased Tuj1$^+$ neurons and that sequential Wnt3a and Wnt5a treatment increased the number of TH$^+$ neurons in VM neurospheres. (*C*) Wnt3a alone increased the percentage of neurons (Tuj1$^+$ cells per field), but Wnt5a alone or in combination with Wnt3a had no effect, and the effect of Wnt3a was reversed by sequential administration of Wnt5a. (*D*) Although neither Wnt3a nor Wnt5a significantly increased the percentage of TH$^+$ neurons out of the total cells in the culture, sequential administration of Wnt3a and Wnt5a greatly increased the percentage of TH$^+$/DAPI cells. (*E*) Although Wnt3a had no effect, Wnt5a increased the percentage of TH$^+$ cells per Tuj1$^+$ area, and sequential Wnt3a and Wnt5a treatment increase this percentage to a greater extent. $^*P < 0.05$ and $^{**}P < 0.01$ ($n$ = 3–4).

*Top*, and *C*), as expected from the antiproliferative effect of Wnt5a that we report. We then examined the proportion of TH$^+$ cells in the cultures and found that only the sequential Wnt3a and Wnt5a treatment induced a significant increase in the number of TH$^+$ cells (Fig. 3*B*, *Middle*, and *D*), also as expected from their sequential effects on progenitor expansion and DA differentiation. Interestingly, when the proportion of DA neurons per Tuj1-stained area was examined, Wnt3a had no significant effect, Wnt5a showed a small increase, and sequential administration of Wnt3a and Wnt5a increased the proportion of DA neurons by 2.5-fold compared with Wnt3a (Fig. 3*B*, *Bottom*, and *E*). Thus, our results show that when Wnt signals are combined sequentially to increase progenitor proliferation (Wnt3a), and then differentiation (Wnt5a), the percentage of DA neurons derived from midbrain neural stem cell cultures increases significantly. Therefore we next examined whether this sequential Wnt protocol also could improve the DA differentiation of mES cells.

**Wnt3a and Wnt5a Cooperate to Improve DA Neuron Development in ES Cell Cultures.** To adapt the Wnt treatment protocol from neurospheres to mES cell cultures, we shortened each of the three steps (Wnt3a/no Wnt/Wnt5a) from 3 d to 2 d (Fig. 4*A*). These three steps were performed between days 7–13, after the neural-induction step with Noggin on days 1–5 and the first Fgf8/Shh-patterning step on days 5–7 and continued during days 7–13. A final standard differentiation step was included to enhance the

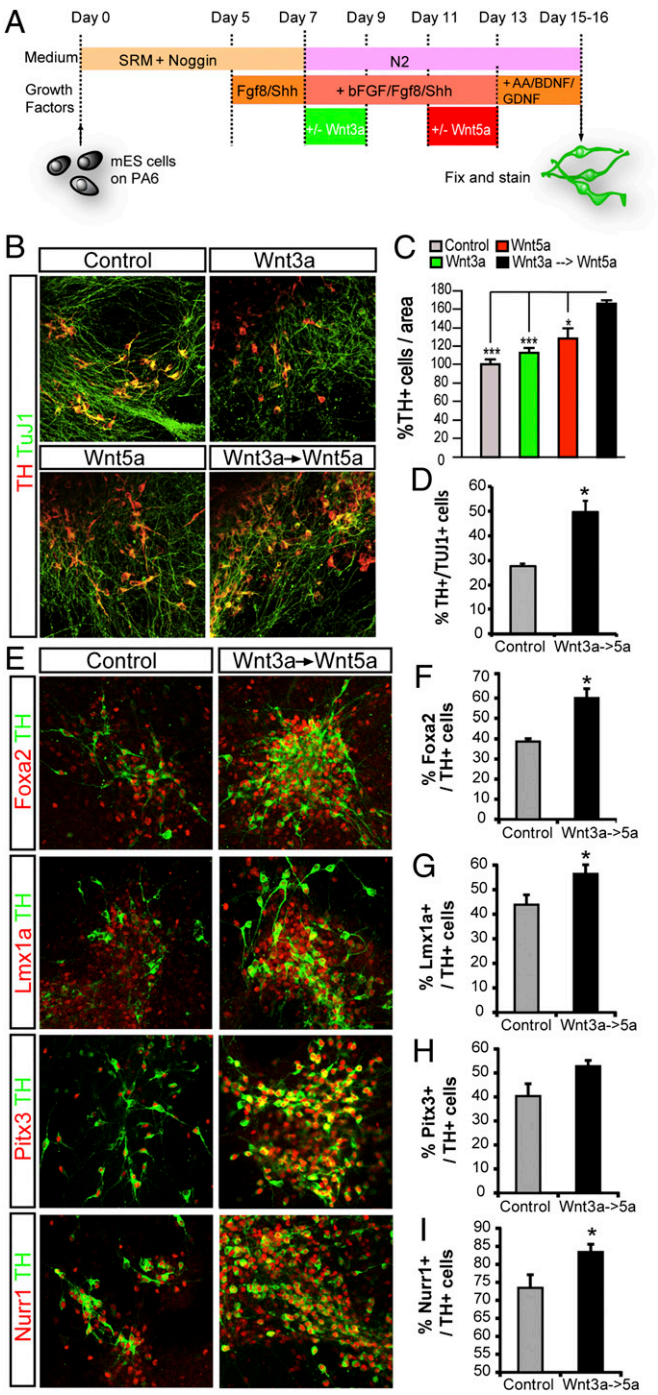


**Fig. 4.** Sequential Wnt3a and Wnt5a treatment improves the midbrain DA differentiation of mES cells. (*A*) ES cells were cultured according to the following scheme: ES cells were neuralized by Noggin (5 d) in SRM and then were patterned with Shh (200 ng/mL) and Fgf8b (25 ng/mL) for 2 d. From days 7–13, cells were grown in N2 containing bFGF (10 ng/mL), Shh, and Fgf8b. From days 13–15/16, cells were differentiated further with ascorbic acid (0.2 mM), BDNF (20 ng/mL), and GDNF (10 ng/mL) before fixation and staining. The effect of Wnt3a was tested by treatment from days 7–9, and the effect of Wnt5a was tested from days 11–13. (*B–D*) Differentiated cells were stained for TH and Tuj1, and the number of $TH^+$ cells was counted. Sequential treatment with Wnt3a and Wnt5a significantly improved the yield of DA neurons by 60% (%$TH^+$ cells per area, *C*) and the proportion of neurons that become $TH^+$ neurons by 80% (%TH/$TUJ1^+$ cells, *D*). (*E–I*) Immunohistochemistry for typical midbrain DA neuron markers such as Foxa2, Lmx1a, Pitx3, and Nurr1 revealed that sequential Wnt3a and Wnt5a treatment induced a tendency for $TH^+$ cells to express Pitx3 (*H*) and a significant increase in the number of $TH^+$ cells that express Foxa2 (*F*), Lmx1a, (*G*), and Nurr1 (*I*). These results indicate that sequential Wnt3a and Wnt5a treatment improves not only the number of $TH^+$ DA neurons but also the acquisition of a midbrain DA neuron phenotype. $^*P < 0.05$, $^{***}P < 0.001$, $n = 3–4$.

maturation of DA neurons on days 13–15/16. As observed with neural stem cells, treatment of mES cells with Wnt3a had no effect on the number of $TH^+$ cells in the cultures. Although Wnt5a was not as efficacious as in ES cultures treated for longer time (14, 17, 26, 44), sequential administration of Wnt3a followed by Wnt5a led to a very significant (60%) increase in the percentage of $TH^+$ cells compared with control or Wnt3a alone (Fig. 4 *B* and *C*). Additionally, sequential Wnt3a and Wnt5a treatment also increased by 80% the proportion of $TuJ1^+$ neurons that became $TH^+$ (Fig. 4*D*). Finally, we examined whether such $TH^+$ cells acquired the expression of appropriate midbrain DA markers such as Foxa2, Lmx1a, Pitx3, and Nurr1 (Fig. 4*E*). Importantly, sequential Wnt treatment increased the proportion of $TH^+$ cells expressing Foxa2 by 55%, Lmx1a by 29%, Pitx3 by 31%, and Nurr1 by 14% (Fig. 4 *F–I*). Thus, our results indicate that, by improving our understanding of the basic mechanisms by which Wnts operate during normal midbrain development, it is possible to improve current protocols for the DA differentiation of neural or ES cells.

## Discussion

In this study we provide evidence that Wnt1 and Wnt5a cooperate at multiple levels, with both synergistic and antagonistic actions, to orchestrate the development of midbrain DA neurons. Earlier studies have shown a role for *Wnt1* in the specification of the DA domain by regulating the expression of *Otx2* and *Nkx2.2* (22). However, it was not known whether *Wnt1* regulates the expression and function of critical factors required for DA neuron specification, such as *Lmx1a* (36), and for DA neurogenesis, such as *Ngn2* and *Mash1* (38). Our data indicate that the specification and neurogenic potential of the midbrain FP are lost in the $Wnt1^{-/-}$ mice, as evidenced by the loss of Lmx1a, *Ngn2*, and *Mash1* expression, the reduced number and proliferation of progenitor cells, and the absence of postmitotic ($Nurr1^+$, $TuJ1^+$, and $TH^+$) cells in the FP. Previous work has implicated Wnt1 in an Lmx1a–Wnt1 autoregulatory loop that controls the expression of Pitx3 and Nurr1 as well as the development of midbrain DA neurons in vitro (23). We show here that Wnt1 is required not only to regulate the expression levels of Lmx1a, Ngn2, Nurr1, and TH in vivo but also to control the appropriate number of cells expressing such markers and is absolutely required for their presence in the midbrain FP. Indeed, in the $Wnt1^{-/-}$ background, all cells in the DA lineage examined, from progenitors ($Lmx1a^+$ and $Ngn2^+$ cells) to postmitotic cells ($Nurr1^+$ and $TH^+$), were absent from the FP and were found ectopically in the BP. Further, this reduced number of $Lmx1a^+$ progenitors found in the BP was displaced laterally to a domain that was capable of generating only a few $Nurr1^+$ precursors and did not allow their efficient differentiation into $TH^+$ DA neurons. Thus, our results identify *Wnt1* as the Wnt required for the correct specification of the FP and DA progenitors, as well as for DA neurogenesis.

Our analysis of $Wnt1^{-/-};Wnt5a^{-/-}$ mice revealed additional contributions of Wnt1 in the regulation of typical Wnt5a-dependent functions, and vice-versa. These results were unexpected, because Wnt1 and Wnt5a are known to activate distinct Wnt signaling pathways—Wnt/β-catenin and Wnt/PCP, respectively—in midbrain DA neurons. However, Wnt signaling components shared by Wnt/β-catenin and Wnt/PCP signaling pathways, such as Fz or Dvl, could contribute to integrate signaling events initiated by Wnt1 or Wnt5a. Moreover, we and others have reported previously that signaling components

initially assigned to the Wnt/β-catenin pathway, such as the Lrp6 coreceptor, can contribute to convergent extension and Wnt/PCP signaling (45, 46). Thus, multiple mechanisms could account for the interaction between these two pathways. In our study, we found that deletion of *Wnt1* worsened all typical Wnt/PCP morphogenesis phenotypes found in *Wnt5a*$^{-/-}$ mice: increased mediolateral and dorsoventral distribution of DA neurons in the VM, and severe A–P shortening of the TH$^{+}$ domain. These data indicated that *Wnt1* cooperates with *Wnt5a* to regulate Wnt5a/PCP-dependent functions in the developing VM. We also found that deletion of *Wnt5a* worsened *Wnt1*$^{-/-}$ phenotypes, such as the decrease in DA neurogenesis and differentiation, as shown by a greater decrease in both Nurr1$^{+}$ and TH$^{+}$ cells in vivo. This result also was unexpected, because deletion of *Wnt5a* partially rescues the proliferation defect in *Wnt1*$^{-/-}$ mice (this study) and increases the number of Nurr1$^{+}$ cells (17). Thus, the analysis of *Wnt1*$^{-/-}$*Wnt5a*$^{-/-}$ mice uncovered two cooperative functions of Wnt1 and Wnt5a, whereby Wnt1 contributes to Wnt5a-dependent morphogenesis and Wnt5a contributes to Wnt1-dependent neurogenesis.

*Shh* and *Fgf8* have been described previously as being expressed at the cross-section between the FP and isthmus and have been demonstrated to regulate the development of VM DA neurons in a coordinated manner (47, 48) and to promote the differentiation of stem cells into midbrain DA neurons (28, 32, 44, 49–51). Similarly, Wnt1 and Wnt5a are coexpressed and intersect in defined spatial and temporal patterns in the developing midbrain: *Wnt1* is expressed in the midbrain as early as E8 (52) and is found in two lateral bands flanking the FP from E10.5–12.5 (22), and *Wnt5a* is expressed in the VM, including the FP, from E9.5–13.5 (17). In this context, our study showing that Wnt1 and Wnt5a cooperate to promote DA neuron development provides the in vivo functional basis for the molecular intersection between Wnt1/β-catenin signaling and Wnt5a/PCP signaling. These findings led us to propose that intersections between Wnts, Shh, and Fgf8, are key elements of the molecular morphogen logic that controls the development of midbrain DA neurons. This concept was tested further and verified in stem cell cultures, where we found that the combined administration of these factors improved the DA differentiation of neural stem and ES cells. In our protocol, in addition to Shh and Fgf8b, we used Wnt3a to activate Wnt/β-catenin signaling, followed by Wnt5a to activate Wnt/PCP signaling. Previous data in the literature have shown that Wnt3a promotes proliferation of neural stem cells and DA progenitors (14, 53) and that activation of Wnt/β-catenin signaling with GSK3β inhibitors enhances DA neurogenesis in DA progenitors (24), mES cells (32), and human ES cells (28). In addition, Wnt5a treatment has been found to inhibit proliferation and to promote DA differentiation of rodent neural and ES cells (14, 17, 26, 44). To date, however, a combined treatment providing adequate temporal activation of both pathways has not been developed. Our results show that appropriate temporal and sequential administration of Wnts successfully improves the DA differentiation of VM neural stem cells, grown as neurospheres, and of ES cells. Sequential Wnt3a and Wnt5a treatment increased the percentage of TH$^{+}$ neurons in midbrain neurosphere cultures. We also found that sequential Wnt treatment increased the number of ES cells that differentiate into TH$^{+}$ cells and acquire expression of transcription factors critical for midbrain DA neuron development, such as Foxa2, Lmx1a, Pitx3, and Nurr1. These results confirmed that sequential Wnt3a and Wnt5a treatment promoted DA differentiation and the acquisition of a true midbrain DA neuron phenotype. Thus, our data suggest that it is possible to replace Wnt1 by Wnt3a, at least partially, to activate β-catenin signaling and promote DA progenitor proliferation. Future availability of purified and active Wnt1 protein will allow testing to determine whether Wnt1 protein may offer additional improvements in DA differentiation protocols, as compared with Wnt3a.

The positive results obtained with neural and ES cells support the idea that Wnt proteins could be used for therapeutic purposes, as previously suggested for hematopoietic stem cells (43). In the case of DA neurons, the main therapeutic target would be Parkinson's disease, a neurodegenerative disorder resulting in the demise of adult midbrain DA neurons. The implementation of protocols such as the one described here for the generation of midbrain DA neurons from stem cells thus may be useful for cell-replacement therapy (54, 55) and in assays for drug discovery, taking advantage of either human ES cells or patient-derived induced pluripotent stem cells (56–58).

In sum, our study identifies a genetic interaction between *Wnt1* and *Wnt5a*, that controls different stages of midbrain DA neuron development in an antagonistic or cooperative manner. Although Wnt1 and Wnt5a competed to promote or inhibit DA progenitor proliferation, respectively, Wnt1 cooperated with Wnt5a in regulating morphogenesis, and Wnt5a collaborated with Wnt1 to promote DA neurogenesis. Importantly, these concepts allowed us to improve current protocols for the DA differentiation of stem cells, opening the door for the development of novel therapies for Parkinson's disease.

## Materials and Methods

**Animals, Immunohistochemistry, and ISH.** *Wnt1*$^{+/-}$ (21), *Wnt5a*$^{+/-}$ (39), Wnt11$^{-/-}$ (59), and CD1 mice (Charles River) were housed, bred, and treated in accordance with protocols approved by the local ethics committees (Stockholm's Norra Djurförsöketiska Nämnd N154/06, N135/08, N145/09, and N273/11). All mutant mice were kept on a C57bl/6 background. *Wnt1*$^{+/-}$ mice were bred with *Wnt5a*$^{+/-}$ mice to generate Wnt1$^{+/-}$Wnt5a$^{+/-}$ mice, which were obtained at the expected Mendelian proportions (expected = 25%, actual = 24.86%, $n$ = 185). For embryo analyses, heterozygous mice of the relevant genotype were mated overnight, and noon of the day the plug was considered E0.5. Embryos were dissected out of the uterine horns in ice-cold PBS, fixed in 4% (wt/wt) paraformaldehyde (PFA) for 4 h to overnight, cryoprotected in 20–30% sucrose, and frozen in Tissue-Tek Optimum Cutting Temperature (OCT) compound (Sakura Fine-Tek) on dry ice. Serial coronal 14-μm sections of the brain were obtained on a cryostat. Immunohistochemistry and ISH were carried out as previously described (14). Probes and antibodies are described below. Immunohistochemistry and ISH were visualized with a Zeiss HBO100 microscope or Zeiss LSM 510 Confocal Microscope, collected with a C4742-95 Hamamatsu camera, and processed with OpenLab software (PerkinElmer), Photoshop (Adobe), and/or ImageJ (http://imagej.nih.gov/ij/). Figures were assembled in Illustrator (Adobe).

**Antibodies and Probes.** The RNA probes for *Shh* (60), *Foxa2* (17), and *Ngn2* and *Mash1* (38) have been described previously.

Rabbit anti-Nurr1 (Nr4a2) (1:1,000; Santa Cruz Biotechnology), rabbit anti-TH (1:500–2000; Pel-Freeze), rabbit anti–phospho-histone3 (1:400; Cell Signaling), mouse anti-β III tubulin (1:1,000–1:2,000; Promega), anti-Foxa2 [1:20; 4C7; Developmental Studies Hybridoma Bank (DSHB)], anti-Nkx6.1 (F55A10; DSHB), anti-Lmx1a (1:1,000; gift from Mike German, University of California, San Francisco, CA), anti-Sox2 (1:500; Millipore), anti-Wnt5a (1:250; R&D Systems), and Cy2-, Cy3-, or Rhodamine-coupled secondary antibodies (1:250; Jackson ImmunoResearch) were used. Some sections or cells were counterstained with DAPI (500 ng/mL) (Sigma), Topro3 (Invitrogen), or Alexa 488 phalloidin (Molecular Probes, Invitrogen).

**Quantification of TH$^{+}$ or Nurr1$^{+}$ Cells in Knockout Mice.** E11.5 and E12.5 brains were sectioned serially at 14 μm to two slides. Because both anti-TH and anti-Nurr1 are rabbit antibodies, one slide was stained for TH and the other for Nurr1. TH$^{+}$ cells were counted in every second 14-μm section (i.e., every 28 μm) through the entire mesodiencephalon from anterior to posterior, and the total number of TH$^{+}$ cells was calculated by multiplying the cell counts by 2. On average, 18 sections per WT slide contained TH$^{+}$ cells, whereas *Wnt1*$^{-/-}$*Wnt5a*$^{+/+}$ and *Wnt1*$^{-/-}$*Wnt5a*$^{+/-}$ slides contained eight sections with TH$^{+}$ cells, and *Wnt1*$^{-/-}$*Wnt5a*$^{-/-}$ slides contained two or three sections with TH$^{+}$ cells. Because Nurr1 is expressed further anteriorly and posteriorly than TH, Nurr1$^{+}$ cells were counted in three sections per brain (28 μm apart) within the central segment of the Th$^{+}$ domain in each genotype. The total number of Nurr1$^{+}$ cells then was calculated by correcting for the total number of

sections containing TH$^+$ DA neurons. All values represent the mean of three or four animals per genotype, ± SEM.

**Statistical Analyses in Knockout Mice.** Statistical analysis was performed with GraphPad Prism. Differences between knockout animals or culture conditions were analyzed using ANOVA, with Bonferroni's post hoc test. Significant differences were assumed at $*P < 0.05$, $**P < 0.01$, and $***P < 0.001$. GraphPad Prism (GraphPad Software) was used for statistical analyses.

**Neurosphere Cultures.** Mouse E11.5 ventral midbrain tissue was dissected out in ice-cold PBS/0.2% glucose. The tissue was dissociated in N2 medium (MEM, F12 medium, Hepes, N2 supplement and Glutamine, all from Life Technologies) by trituration through flame-narrowed Pasteur pipettes. The cell suspension then was plated at $1 \times 10^5$ cells/cm$^2$ (100,000 cells/mL) on uncoated Petri flasks (BD Falcon) in complete medium consisting of 200–300 ng/mL Shh (R&D Systems), 25 ng/mL FGF8b (R&D Systems), and 20 ng/mL basis FGF (bFGF; R&D Systems) in N2. The design of the experiments using Wnt3a and/or Wnt5a in neurospheres was as follows: First, neurospheres were cultured with or without Wnt3a (100–300 ng/mL) (R&D Systems) in N2 with Shh, FGF8, and bFGF. After 3 d, cells were collected, washed with Wnt vehicle (CHAPS 0.05%; Tamro), and plated at a density of 100,000 cells/mL without adding Wnts. After a second passage, cells were plated and differentiated with or without Wnt5a (100 ng/mL) (R&D Systems) (see scheme in Fig. 3*A*). At day 9, cells were fixed in 4% (wt/vol) PFA and processed for immunocytochemistry as described below.

**ES Cell Culture.** mES R1cell cultures were cultured on gelatinized plates in KO-DMEM (Life Technologies) supplemented with 15% (vol/vol) Knockout serum replacement (SRM; Life Technologies), 2 mM L-glutamine (Life Technologies), 1% nonessential amino acids (VWR), 0.1 mM β-mercaptoethanol (Sigma), 1,000 U/mL leukemia inhibitory factor (ESGRO; Chemicon/Millipore), and 10,000 U/mL penicillin/streptomycin (Life Technologies). Stromal PA6 cells were cultured in α-minimum essential medium (Life Technologies) containing 10% (vol/vol) FBS (Life Technologies), 2 mM L-glutamine (Life Technologies), and 10,000 U/mL penicillin/streptomycin (Life Technologies) and were mitotically inactivated before use with 1 μg/mL mitomycin C (Roche) overnight at 37 °C. All cell lines were maintained at 37 °C, 5% $CO_2$ and 95% humidity. mES cells were plated at low density (100 cells/cm$^2$) on a confluent layer of PA6 cells in 24-well plates and were grown in SRM and Noggin (300 ng/mL; R&D Systems). At day 5, 200 ng/mL Shh and 25 ng/mL FGF8b were added to the medium. After 7 d, cultures were switched to N2 medium in the presence of Shh, FGF8, and FGF2 (10 ng/mL), with or without 100 ng/mL Wnt3a (R&D Systems). At day 9, Wnt3a was withdrawn, cells were washed with CHAPS for 1 h, and fresh medium was added. Two days later (on day 11) 100 ng/mL Wnt5a (R&D Systems) was added with fresh medium. Four conditions were tested: (*a*) control with no Wnt addition; (*b*) Wnt3a alone added at day 7 and then removed at day 9; (*c*) Wnt5a alone added from days 11–13; and (*d*) Wnt3a added at day 7, cells washed at day 9, and Wnt5a added from days 11–13. Shh, FGF8, bFGF, and Wnt5a were removed at day 13 from the conditions in which they had been added. Cultures then were differentiated until day 15 in N2 medium containing 0.2 mM ascorbic acid, 20 ng/mL BDNF (R&D Systems), and 10 ng/mL glial cell-derived neurotrophic factor (GDNF; R&D Systems). At day 15 cells were fixed in 4% PFA and processed for immunocytochemistry as described below.

**Immunocytochemistry.** PFA-fixed cells were washed in PBS and blocked in 5% (vol/vol) normal goat serum/PBS for 1 h at room temperature. Primary antibodies were diluted in PBS (pH 7.4), 0.3% Triton X-100, and 1% (wt/vol) BSA, and incubations were carried out overnight at 4 °C. After washes, incubations with the appropriate Alexa-conjugated secondary antibodies (1:500; Life Technologies) were carried out for 2 h at room temperature. The following antibodies were used: mouse monoclonal anti–β-tubulin III (TuJ1) (1:1,000; Promega), rabbit polyclonal anti-TH (1:500; Pel-Freeze) or mouse monoclonal anti-TH (1:500; Sigma or 1:400; Immunostar), rabbit polyclonal anti-Nurr1 (1:250; Santa Cruz), rabbit polyclonal anti-Pitx3 (1:50; Invitrogen), rabbit polyclonal anti-Lmx1a (1:500; a gift from M. German), and rabbit polyclonal anti-Foxa2 (1:500; Cell Signaling Technology).

**Cell Counts in Vitro.** For neurosphere cultures, Hoechst staining (Roche) was used and TH$^+$, Tuj1$^+$, and Hoechst-positive cells were counted in 10–12 predetermined fields along the *x* axis of the well. For each field, up to nine z-planes were analyzed. Each condition was analyzed in duplicate to quadruplicate determinations for every experiment, and three to four independent experiments were performed for every condition.

For ES cell cultures, TH$^+$ cells per area were counted in 12 colonies per well, in three wells per condition, and in four independent experiments. To correct for variations in colony size, the number of TH$^+$ cells was referred to the area occupied by the colonies. The percentage of TH$^+$/Tuj1$^+$ cells also was counted in 8–10 fields along the *x* axis of the well in two wells per experiment and three experiments per condition. Finally, the number of TH$^+$ cells expressing midbrain DA markers (Foxa2, Lmx1a, Pitx3, and Nurr1) was counted in 8–12 fields, in duplicate wells and three independent experiments.

All data are expressed as mean ± SEM. Statistical analysis was performed by *t*-test or ANOVA with post hoc tests.

**Wnt Signaling.** SN4741 cells were transfected with 500 ng SuperTOP-FLASH/SuperFOP-FLASH and 50 ng of Renilla-expressing vector pRL-TK Luc (Promega) using Superfect (Qiagen) according to the manufacturer's instructions. Twelve hours after transfection, cells were stimulated with 50–100 ng/mL recombinant Wnt3a (R&D Systems) and/or 50–500ng/mL Wnt1 (Preprotech) for 24 h. Reporter activity was measured using the Dual-Luciferase Reporter assay (Promega). Each experiment was repeated three times, and each experimental condition was measured in duplicate. Background luminescence (signal from lysis buffer without any cells) was subtracted from each sample. Luciferase activity of SuperTOP/FOP-FLASH was normalized to Renilla luciferase signal.

Sample preparation, Western blot analysis, and signal detection was performed as previously described (61). Primary antibodies used were rabbit polyclonal anti-Phospho-LRP5/6 (1:1,000; Cell Signaling), mouse monoclonal anti–β-actin (1:5,000; BD Transduction Laboratories), and mouse monoclonal anti–active β-catenin (1:1,000; Millipore). HRP-conjugated anti-mouse and anti-rabbit secondary antibodies, A7282 and A6667 respectively, were purchased from Sigma, and were used at 1:5,000.

**ACKNOWLEDGMENTS.** This work was supported by grants from the Swedish Foundation for Strategic Research (Center of Excellence in Developmental Biology and Successful Research Leaders Program); Swedish Research Council Grants VR2008:2811, VR2008:3287, and VR2011:3116; the Center of Excellence in Developmental Biology for Regenerative Medicine); the Karolinska Institute (Thematic Center in Stem Cells and Regenerative Medicine); the European Commission (Neurostemcell and DDPD-Genes); and Parkinsonfonden. J.C.V. was supported by a Federation of European Biochemical Societies Long-Term Fellowship. V.B. is supported by the Czech Science Foundation (204/09/0498, 301/11/0747).

1. Chien AJ, Conrad WH, Moon RT (2009) A Wnt survival guide: From flies to human disease. *J Invest Dermatol* 129(7):1614–1627.
2. Sugimura R, Li L (2010) Noncanonical Wnt signaling in vertebrate development, stem cells, and diseases. *Birth Defects Res C Embryo Today* 90(4):243–256.
3. Inestrosa NC, Arenas E (2010) Emerging roles of Wnts in the adult nervous system. *Nat Rev Neurosci* 11(2):77–86.
4. Grigoryan T, Wend P, Klaus A, Birchmeier W (2008) Deciphering the function of canonical Wnt signals in development and disease: Conditional loss- and gain-of-function mutations of beta-catenin in mice. *Genes Dev* 22(17):2308–2341.
5. Angers S, Moon RT (2009) Proximal events in Wnt signal transduction. *Nat Rev Mol Cell Biol* 10(7):468–477.
6. Wu J, Mlodzik M (2009) A quest for the mechanism regulating global planar cell polarity of tissues. *Trends Cell Biol* 19(7):295–305.
7. Hur EM, Zhou FQ (2010) GSK3 signalling in neural development. *Nat Rev Neurosci* 11(8):539–551.
8. Wu H, Xiong WC, Mei L (2010) To build a synapse: Signaling pathways in neuromuscular junction assembly. *Development* 137(7):1017–1033.
9. Cerpa W, Toledo EM, Varela-Nallar L, Inestrosa NC (2009) The role of Wnt signaling in neuroprotection. *Drug News Perspect* 22(10):579–591.
10. Fradkin LG, Dura JM, Noordermeer JN (2010) Ryks: New partners for Wnts in the developing and regenerating nervous system. *Trends Neurosci* 33(2):84–92.
11. Freese JL, Pino D, Pleasure SJ (2010) Wnt signaling in development and disease. *Neurobiol Dis* 38(2):148–153.
12. Salinas PC, Zou Y (2008) Wnt signaling in neural circuit assembly. *Annu Rev Neurosci* 31:339–358.
13. Rawal N, et al. (2006) Dynamic temporal and cell type-specific expression of Wnt signaling components in the developing midbrain. *Exp Cell Res* 312(9):1626–1636.
14. Castelo-Branco G, et al. (2003) Differential regulation of midbrain dopaminergic neuron development by Wnt-1, Wnt-3a, and Wnt-5a. *Proc Natl Acad Sci USA* 100(22):12747–12752.
15. Fischer T, Guimera J, Wurst W, Prakash N (2007) Distinct but redundant expression of the Frizzled Wnt receptor genes at signaling centers of the developing mouse brain. *Neuroscience* 147(3):693–711.

16. Sousa KM, et al. (2010) Wnt2 regulates progenitor proliferation in the developing ventral midbrain. *J Biol Chem* 285(10):7246–7253.
17. Andersson ER, et al. (2008) Wnt5a regulates ventral midbrain morphogenesis and the development of A9-A10 dopaminergic cells in vivo. *PLoS ONE* 3(10):e3517.
18. Thomas KR, Capecchi MR (1990) Targeted disruption of the murine int-1 proto-oncogene resulting in severe abnormalities in midbrain and cerebellar development. *Nature* 346(6287):847–850.
19. McMahon AP, Bradley A (1990) The Wnt-1 (int-1) proto-oncogene is required for development of a large region of the mouse brain. *Cell* 62(6):1073–1085.
20. Danielian PS, McMahon AP (1996) Engrailed-1 as a target of the Wnt-1 signalling pathway in vertebrate midbrain development. *Nature* 383(6598):332–334.
21. McMahon AP, Joyner AL, Bradley A, McMahon JA (1992) The midbrain-hindbrain phenotype of Wnt-1-/Wnt-1- mice results from stepwise deletion of engrailed-expressing cells by 9.5 days postcoitum. *Cell* 69(4):581–595.
22. Prakash N, et al. (2006) A Wnt1-regulated genetic network controls the identity and fate of midbrain-dopaminergic progenitors in vivo. *Development* 133(1):89–98.
23. Chung S, et al. (2009) Wnt1-lmx1a forms a novel autoregulatory loop and controls midbrain dopaminergic differentiation synergistically with the SHH-FoxA2 pathway. *Cell Stem Cell* 5(6):646–658.
24. Castelo-Branco G, Rawal N, Arenas E (2004) GSK-3beta inhibition/beta-catenin stabilization in ventral midbrain precursors increases differentiation into dopamine neurons. *J Cell Sci* 117(Pt 24):5731–5737.
25. Rawal N, et al. (2009) Parkin protects dopaminergic neurons from excessive Wnt/beta-catenin signaling. *Biochem Biophys Res Commun* 388(3):473–478.
26. Schulte G, et al. (2005) Purified Wnt-5a increases differentiation of midbrain dopaminergic cells and dishevelled phosphorylation. *J Neurochem* 92(6):1550–1553.
27. Cajánek L, et al. (2009) Wnt/beta-catenin signaling blockade promotes neuronal induction and dopaminergic differentiation in embryonic stem cells. *Stem Cells* 27(12):2917–2927.
28. Kriks S, et al. (2011) Dopamine neurons derived from human ES cells efficiently engraft in animal models of Parkinson's disease. *Nature* 480(7378):547–551.
29. Chilov D, Sinjushina N, Saarimäki-Vire J, Taketo MM, Partanen J (2010) beta-Catenin regulates intercellular signalling networks and cell-type specific transcription in the developing mouse midbrain-rhombomere 1 region. *PLoS ONE* 5(6):e10881.
30. Tang M, Miyamoto Y, Huang EJ (2009) Multiple roles of beta-catenin in controlling the neurogenic niche for midbrain dopamine neurons. *Development* 136(12): 2027–2038.
31. Joksimovic M, et al. (2009) Wnt antagonism of Shh facilitates midbrain floor plate neurogenesis. *Nat Neurosci* 12(2):125–131.
32. Tang M, et al. (2010) Interactions of Wnt/beta-catenin signaling and sonic hedgehog regulate the neurogenesis of ventral midbrain dopamine neurons. *J Neurosci* 30(27): 9280–9291.
33. Hynes M, Poulsen K, Tessier-Lavigne M, Rosenthal A (1995) Control of neuronal diversity by the floor plate: Contact-mediated induction of midbrain dopaminergic neurons. *Cell* 80(1):95–101.
34. Kittappa R, Chang WW, Awatramani RB, McKay RD (2007) The foxa2 gene controls the birth and spontaneous degeneration of dopamine neurons in old age. *PLoS Biol* 5(12):e325.
35. Ferri AL, et al. (2007) Foxa1 and Foxa2 regulate multiple phases of midbrain dopaminergic neuron development in a dosage-dependent manner. *Development* 134(15):2761–2769.
36. Andersson E, et al. (2006) Identification of intrinsic determinants of midbrain dopamine neurons. *Cell* 124(2):393–405.
37. Hynes M, Rosenthal A (1999) Specification of dopaminergic and serotonergic neurons in the vertebrate CNS. *Curr Opin Neurobiol* 9(1):26–36.
38. Kele J, et al. (2006) Neurogenin 2 is required for the development of ventral midbrain dopaminergic neurons. *Development* 133(3):495–505.
39. Yamaguchi TP, Bradley A, McMahon AP, Jones S (1999) A Wnt5a pathway underlies outgrowth of multiple structures in the vertebrate embryo. *Development* 126(6): 1211–1223.
40. Young CS, Kitamura M, Hardy S, Kitajewski J (1998) Wnt-1 induces growth, cytosolic beta-catenin, and Tcf/Lef transcriptional activation in Rat-1 fibroblasts. *Mol Cell Biol* 18(5):2474–2485.
41. Hinck L, Nelson WJ, Papkoff J (1994) Wnt-1 modulates cell-cell adhesion in mammalian cells by stabilizing beta-catenin binding to the cell adhesion protein cadherin. *J Cell Biol* 124(5):729–741.
42. Peifer M, Sweeton D, Casey M, Wieschaus E (1994) wingless signal and Zeste-white 3 kinase trigger opposing changes in the intracellular distribution of Armadillo. *Development* 120(2):369–380.
43. Willert K, et al. (2003) Wnt proteins are lipid-modified and can act as stem cell growth factors. *Nature* 423(6938):448–452.
44. Parish CL, et al. (2008) Wnt5a-treated midbrain neural stem cells improve dopamine cell replacement therapy in parkinsonian mice. *J Clin Invest* 118(1):149–160.
45. Bryja V, et al. (2009) The extracellular domain of Lrp5/6 inhibits noncanonical Wnt signaling in vivo. *Mol Biol Cell* 20(3):924–936.
46. Tahinci E, et al. (2007) Lrp6 is required for convergent extension during Xenopus gastrulation. *Development* 134(22):4095–4106.
47. Hynes M, et al. (1995) Induction of midbrain dopaminergic neurons by Sonic hedgehog. *Neuron* 15(1):35–44.
48. Ye W, Shimamura K, Rubenstein JL, Hynes MA, Rosenthal A (1998) FGF and Shh signals control dopaminergic and serotonergic cell fate in the anterior neural plate. *Cell* 93(5):755–766.
49. Barberi T, et al. (2003) Neural subtype specification of fertilization and nuclear transfer embryonic stem cells and application in parkinsonian mice. *Nat Biotechnol* 21(10):1200–1207.
50. Lonardo E, et al. (2010) A small synthetic cripto blocking Peptide improves neural induction, dopaminergic differentiation, and functional integration of mouse embryonic stem cells in a rat model of Parkinson's disease. *Stem Cells* 28(8): 1326–1337.
51. Sanchez-Pernaute R, et al. (2008) Parthenogenetic dopamine neurons from primate embryonic stem cells restore function in experimental Parkinson's disease. *Brain* 131 (Pt 8):2127–2139.
52. Davis CA, Joyner AL (1988) Expression patterns of the homeo box-containing genes En-1 and En-2 and the proto-oncogene int-1 diverge during mouse development. *Genes Dev* 2(12B):1736–1744.
53. Kalani MY, et al. (2008) Wnt-mediated self-renewal of neural stem/progenitor cells. *Proc Natl Acad Sci USA* 105(44):16970–16975.
54. Arenas E (2010) Towards stem cell replacement therapies for Parkinson's disease. *Biochem Biophys Res Commun* 396(1):152–156.
55. Lindvall O, Kokaia Z (2009) Prospects of stem cell therapy for replacing dopamine neurons in Parkinson's disease. *Trends Pharmacol Sci* 30(5):260–267.
56. Kiskinis E, Eggan K (2010) Progress toward the clinical application of patient-specific pluripotent stem cells. *J Clin Invest* 120(1):51–59.
57. Nguyen HN, et al. (2011) LRRK2 mutant iPSC-derived DA neurons demonstrate increased susceptibility to oxidative stress. *Cell Stem Cell* 8(3):267–280.
58. Soldner F, et al. (2011) Generation of isogenic pluripotent stem cells differing exclusively at two early onset Parkinson point mutations. *Cell* 146(2):318–331.
59. Majumdar A, Vainio S, Kispert A, McMahon J, McMahon AP (2003) Wnt11 and Ret/Gdnf pathways cooperate in regulating ureteric branching during metanephric kidney development. *Development* 130(14):3175–3185.
60. Puelles E, et al. (2004) Otx2 regulates the extent, identity and fate of neuronal progenitor domains in the ventral midbrain. *Development* 131(9):2037–2048.
61. Bryja V, et al. (2005) Abnormal development of mouse embryoid bodies lacking p27Kip1 cell cycle regulator. *Stem Cells* 23(7):965–974.